

A Quantum Chemical Study of Racemization Pathways in Substituted Chrysene Derivatives

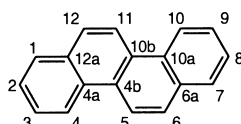
Carsten Kind, Andreas W. Götz, and Bernd A. Hess*^[a]

Abstract: The potential-energy surfaces of 5,11-disubstituted 6,12-dimethoxychrysene and chrysene-6,12-dione derivatives were investigated by means of density functional calculations. We report relative energies of all conformers and an identification of the racemisation pathways of the chiral equilibrium structures. By analysis of homodesmotic reactions we were able to obtain an estimate for the strain energy of the substituted compounds. This strain energy can be used as a means of measuring the steric effects exerted by the substituents.

Keywords: chirality • chrysene • density functional calculations • racemization • transition states

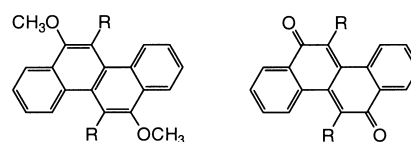
Introduction

During studies of the chromium-mediated benzannulation reaction Dötz et al. discovered 6,12-dimethoxy-5,11-diphenylchrysene (**5**) as one of the products.^[1] Subsequently, the synthesis of 6,12-dimethoxy-5,11-dipropylchrysene (**4**) and 5,11-diphenylchrysene-6,12-dione (**10**) was accomplished by the same group.^[2] For convenience, the usual atom numbering of chrysene is depicted here.



In this work we consider several derivatives of 6,12-dimethoxychrysene and chrysene-6,12-dione that are symmetrically substituted in positions 5 and 11. A characteristic property of these two novel compound classes (**1–5** and **6–10**) is their axial chirality. It has its origin in the steric buttressing effect between the substituents and the adjacent hydrogen atoms, which causes the chrysene core to be twisted.

The racemisation rate of a chiral compound is a most important criterion in the design of a stereoselective synthetic



1 R=H, **2** R=CH₃,
3 R=C₂H₅, **4** R=C₃H₇,
5 R=C₆H₅

6 R=H, **7** R=CH₃,
8 R=C₂H₅, **9** R=C₃H₇,
10 R=C₆H₅

route. It is determined by the largest energy barrier encountered in the racemisation reaction. Therefore conformational stability and strain energy of chiral compounds have been a long-term issue in the literature.

Structures which have been investigated in this context are, for instance, [*n*]helicenes^[3] and *ortho,ortho'*-substituted phenanthrene derivatives.^[4–8] A similar twist of the aromatic core, leading to axial chirality, is observed in these compounds. The chrysene core can be regarded as two nested phenanthrene substructures. Whereas, in the case of *ortho,ortho'*-substituted phenanthrene derivatives, there is only one group of substituents keeping the core twisted, there are two such groups situated on opposite sides of the core in the compounds considered in this work. The term “twisting motion” can be assigned to the movement that converts the scaffold of a distorted phenanthrene or chrysene derivative into its enantiomer and leads to the following question: Does the twisting motion of the chrysene derivatives take place in one step, without intermediates, or in two steps involving an intermediate? In the first case both phenanthrene substructures would have to perform the twisting motion symmetrically at the same time, with the substituents on both sides of the chrysene core passing the adjacent hydrogen atoms simultaneously. In the second case, the phenanthrene substructures

[a] Prof. Dr. B. A. Hess, Dr. C. Kind, Dipl.-Chem. A. W. Götz
Lehrstuhl für Theoretische Chemie
Universität Erlangen-Nürnberg, Egerlandstrasse 3
91058 Erlangen (Germany)
Fax: (+49)9131-8527736
E-mail: hess@chemie.uni-erlangen.de

Supporting information for this article is available on the WWW under <http://www.chemeurj.org/> or from the author.

would have to perform the twisting motion successively, that is with one substituent passing the adjacent hydrogen atom after the other substituent has done so.

A major difference between the two investigated classes of compounds lies in their core. Whereas in one class (**1** to **5**) the aromatic system of the unsubstituted chrysene core is preserved, the core of the other class (**6** to **10**) can be regarded as a quinoid substructure augmented by two isolated benzene rings. Fritsch et al. touch on this aspect in a work about phenanthrenequinone derivatives.^[9] At this point the question arises as to how the strain energy and the energy barrier of the twisting motion are affected by these two different electronic structures.

To contribute to the solution of the aforementioned problems, we set out to explore the conformational manifold of these compounds, to determine the most stable structures and to calculate the energy barriers in the reaction path from one enantiomer to its mirror image. We accomplished these tasks by calculating the equilibrium structures of all stable conformers, by means of density functional theory, and analysing the structural parameters of the lowest energy structure for all considered compounds. The characterisation of the lowest energy structures is completed by an evaluation of the effects of the electronic structure of the core on the structural parameters. This is achieved by analysis of the strain energy, which is defined through homodesmotic reactions. For identification of the racemisation pathways and determination of the associated energy barriers, a topological map containing all conformers and interconnecting transition states can be drawn for each compound. We present only those topological maps that could be reduced to a two-dimensional picture. The topology of the potential surface of the higher alkyl analogues can be derived from the lower ones, since the additional degrees of freedom, that is, rotations around C–C bonds of the alkyl groups, are not strongly coupled to the twisting motion. For one exemplary case we performed single-point second-order Møller–Plesset calculations to check for the reliability of the energy barriers obtained by the density functional calculations.

Computational Methods

For all calculations we used the density functional and second-order Møller–Plesset (MP2) program packages provided by the TURBOMOLE 5.1 suite of programs.^[10] The employed density functionals are the Becke–Perdew BP86^[11, 12] and the hybrid functional B3LYP^[13], as implemented in TURBOMOLE. The resolution of identity (RI) technique was employed to accelerate the BP86^[14, 15] and MP2 calculations.^[16, 17] We used exclusively the TZVP basis set—triple zeta basis plus polarisation functions on all atoms^[18]—which, in a previous work, was shown to be a minimum requirement for performing a reliable force constants analysis.^[19] Accurately converged SCF (self consistent field) results (a termination threshold of at least 10^{-8} a.u. for the total energy) were used to guarantee satisfactory accuracy of the force constants. The force constants were obtained as numerical first derivatives of energy gradients (provided by the TURBOMOLE programs grad and rdgrad), as implemented in a parallel PVM code developed by S. Grimme and M. Gastreich^[20] and extended by B. A. Heß, C. Kind, M. Reiher and J. Neugebauer.^[21] A modified version of MOPAC-6.0, with the ability to use TURBOMOLE programs for energy and gradient calculations, was used for transition state searches. In the case of failure of available methods such as eigenvector

following, we scanned along promising dihedral angles to lead to the transition state of interest, while relaxing all other coordinates. For this purpose we developed the program ROTCURVE,^[22] which uses the modified MOPAC (which, in turn, uses TURBOMOLE) for constrained geometry optimisations. This program was also used to provide data for the two-dimensional potential-energy-surface cuts presented below in the section dealing with analysis of strain energy. All structures were verified to be minima or transition states on the potential-energy surface by means of force constants analysis. Cartesian coordinates of all minima and transition-state structures obtained with both functionals are given as Supporting Information.

The visualisation of the molecular structures given in Figures 1, 2, 4 and 7 was accomplished by means of the MOLDEN program.^[23]

Results

Equilibrium structures: The most stable conformer of each investigated derivative of 6,12-dimethoxychrysene and chrysene-6,12-dione is shown in Figure 1. For every structure, the lowest energy conformation found in the scanned conformational space turns out to have C_2 symmetry. The reason becomes evident when considering a fictitious conformer with C_{2h} symmetry that has to be planar. Bending the substituents (or twisting the core) symmetrically out of plane to minimise the steric hindrance of the substituents leads to structures with C_2 or C_i symmetry. Bending both substituents towards the same side of the plane leads to a reduction to C_2 symmetry and the resulting structures have a strongly twisted chrysene core (cf. Figure 1). Rotation of substituents leads to conformations with further reduced symmetry. Bending them to opposite sides leads to C_i -symmetrical structures with an essentially planar core. These can be regarded as intermediates of a twisting motion that is carried out in two steps starting from a strongly twisted, low-energy conformer. In other words, they result from a twisting motion of one of the phenanthrene substructures starting from the most stable conformers. Structures with such planar cores will be denoted “semitwisted” in the following. One example of a semitwisted equilibrium structure for each compound class is shown in Figure 2, demonstrating the difference of the twist of the chrysene core in comparison to the C_2 -symmetrical lowest-energy conformers. In some cases, semitwisted structures turned out to be transition states (verified by frequency analysis). Consequently, they can be regarded as the transition states of a twisting motion that is carried out in one step, that is, they result from a simultaneous twisting motion of both phenanthrene substructures.

Analysis of the structural parameters of the most stable conformers: For the discussion of the twist of the molecular framework we are going to employ the dihedral angles given in Table 1. The angles C5–C4b–C10b–C11 and C4a–C4b–C10b–C10a adopt values of 140 – 160° and 150 – 160° , respectively, for the lowest energy conformers, and are exactly 180° for the C_i -symmetrical structures. The dihedral angle C4–C4a–C4b–C5 is a direct measurement of the distortion caused by the steric hindrance of the substituent R and the adjacent hydrogen atom. In addition, it can be used for comparison with results obtained by Grimme^[4] on the equivalent angle in phenanthrene derivatives.

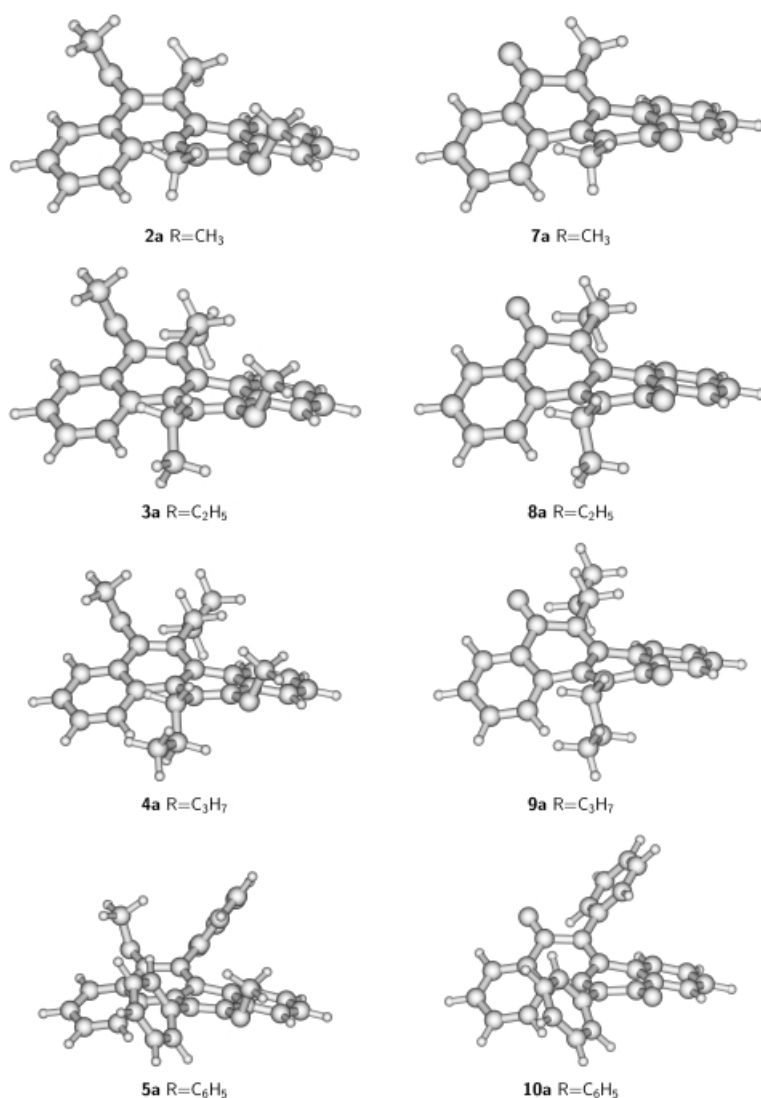


Figure 1. Equilibrium structures of the most stable conformers (indicated by **a**) of the 6,12-dimethoxychrysene (left) and the analogous chrysene-6,12-dione derivatives (right).

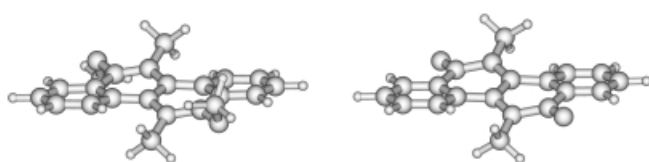


Figure 2. C_2 -symmetrical conformers of 6,12-dimethoxy-5,11-dimethylchrysene (**2d**, left) and 5,11-dimethylchrysene-6,12-dione (**7b**, right).

We find that the dependence of the bond lengths and angles on the applied density functional is small. However, it should be noted that we observed a larger variety of stable conformers and more strongly twisted structures in preliminary empirical forcefield and semiempirical studies. These simple models are not appropriate for investigation of these classes of compounds. Thus we also find it instructive to present the structural parameters both for the BP86 as well as the B3LYP functional. A closer look at the values shows that the structural parameters of the chrysene-6,12-dione derivatives depend more sensitively on the applied functional. The

B3LYP functional tends to predict structures that are slightly more distorted from planarity than does the BP86 functional.

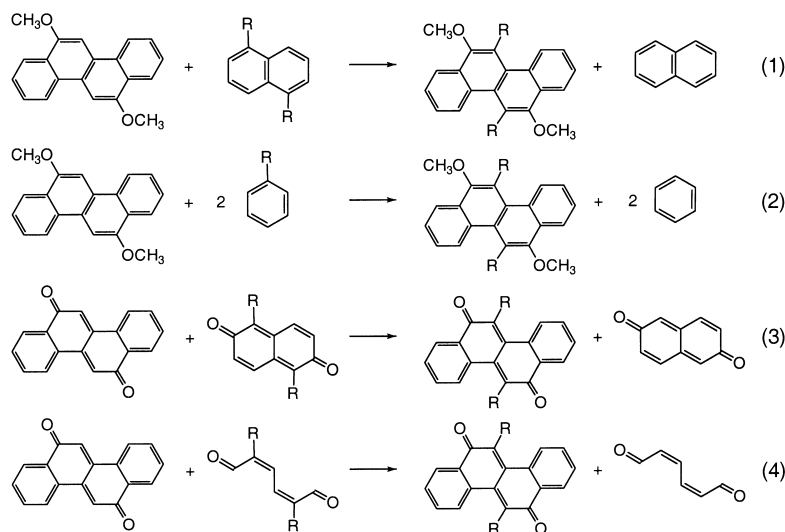
The only compound found to be completely planar, and thus showing C_{2h} symmetry, is 6,12-dimethoxychrysene. We attribute this to the aromaticity of the chrysene core, since the unsubstituted chrysene-6,12-dione shows a slightly twisted C_2 -symmetrical structure, even though the oxo group is sterically less demanding than the methoxy group. In general, the aromatic system tends to maintain a planar structure. In the absence of the aromatic system, that is, in the quinoid structures of the chrysene-6,12-dione derivatives, this tendency is not so pronounced. This is evidently the reason for the stronger twist of the chrysene-6,12-dione derivatives relative to the corresponding 6,12-dimethoxychrysene derivatives. The twist of the chrysene core of the dimethyl derivatives is very similar to that of the higher homologues. As expected, the difference between diethyl and dipropyl derivatives is negligible and similar structural parameters can thus be expected for higher homologues. The calculated values compare well with experimental results,^[2]

which for convenience are also listed in Table 1. For **10a** the agreement is very good (within $1-2^\circ$ for the dihedral angles); we attribute the slightly worse ($2-4^\circ$) agreement in the case of **4a** to interactions of the bulky substituents in the lattice, which are not considered in the calculation.

Analysis of the strain energy: The strain energy that is introduced into compounds **1** and **6** by replacement of the hydrogen atoms at the 5- and 11-positions by a substituent can be expressed using homodesmotic reactions.^[24] We define the strain energy as the energy that is necessary to exchange two substituents from an unstrained reference system with the hydrogen atoms at the 5- and 11-positions of 6,12-dimethoxychrysene and chrysene-6,12-dione, respectively (Scheme 1). 1,5-Disubstituted naphthalene derivatives would seem to be an obvious choice to use as reference compounds for the chrysene derivatives **2** to **5**, especially because naphthalene should represent the electronic structure of the chrysene core quite well. On the other hand, a steric interaction of the substituents at the 1- and 5-positions with the hydrogen atoms

Table 1. Selected dihedral angles for the lowest-energy conformers of the chrysene-6,12-dione and 6,12-dimethoxychrysene derivatives optimised with the BP86/RI and the B3LYP method. Experimental values are taken from literature.^[2]

		C5-C4b-C10b-C11	C4a-C4b-C10b-C10a	C4-C4a-C4b-C5	C4a-C4b-C10b-C11
6,12-dimethoxychrysene derivatives					
1	BP86	180.0	180.0	0.0	0.0
	B3LYP	180.0	180.0	0.0	0.0
2a	BP86	154.9	159.6	25.0	22.7
	B3LYP	155.2	159.2	24.7	22.8
3a	BP86	153.4	160.5	27.4	23.1
	B3LYP	153.3	160.1	27.4	23.2
4a	BP86	153.3	160.5	26.9	23.0
	B3LYP	153.6	160.3	27.2	23.0
5a	exptl.	157.8	162.5	–	19.0/19.9
	BP86	159.4	158.1	19.3	21.3
	B3LYP	159.0	158.1	19.8	21.5
chrysene-6,12-dione derivatives					
6	BP86	167.9	173.6	11.3	9.3
	B3LYP	167.4	173.3	11.9	9.7
7a	BP86	145.3	157.4	33.8	28.7
	B3LYP	144.2	156.3	34.8	29.7
8a	BP86	144.0	157.4	36.0	29.3
	B3LYP	142.7	156.2	37.3	30.5
9a	BP86	144.1	157.7	35.8	29.1
	B3LYP	143.0	156.4	37.0	30.3
10a	BP86	146.5	154.4	31.0	29.6
	B3LYP	145.2	154.2	33.0	30.3
	exptl.	147.3	152.2	–	29.8/30.7



Scheme 1. Homodesmotic reactions used to estimate the strain energy in the 5,11-disubstituted 6,12-dimethoxychrysene [reactions (1) and (2)] and chrysene-6,12-dione [reactions (3) and (4)] derivatives. Results are reported in Table 2.

at 8- and 4-positions, respectively, in the naphthalene derivatives cannot be excluded. To investigate this more closely and as a test of the consistency of the results, monosubstituted benzene derivatives were used as a second type of reference system. The reference of choice for the chrysenedione derivatives **7** to **10** are 1,5-disubstituted 2,6-naphthalenedione derivatives, as they should also faithfully represent the electronic structure of the chrysenedione core. Again, however, we face the problem that steric interaction of the substituents at the 1- and 5-positions with the hydrogen atoms at the 8- and 4-positions in the 2,6-naphthalenedione deriv-

atives cannot be excluded. Thus 2,5-disubstituted (*Z,Z*)-2,4-hexadienedial derivatives were employed as a second reference system to assert the consistency of the results. The energetics for the homodesmotic reactions (1) to (4) depicted in Scheme 1 are summarised in Table 2.

As expected there are no significant differences between the energies obtained with the BP86 and B3LYP functionals. The energy difference between reactions (1) and (2) lies in the range of 5–20 kJ mol⁻¹ and is of the order of 10 kJ mol⁻¹ for reactions (3) and (4). This finding confirms the proposition that the reference systems of reactions (1) and (3) are not completely strain free. Nevertheless, both reactions (3) and (4) and also, apart from structure **5a**, reactions (1) and (2) show the same trend for the strain energy of the investigated compounds. There does not seem to be a large dependence of the strain energy on the substituent. The most striking observation to be made is that the chrysene-6,12-dione derivatives have two to three times lower strain energies than the corresponding 6,12-dimethoxychrysene derivatives. The aromatic system of the core of the latter compounds can account for this. The balance between lower steric hindrance and loss of aromatic stabilisation by an increasing twist of the chrysene core is the reason for the observed high strain energy. In order to support this statement we analysed two-dimensional cuts of the potential-energy surface of chrysene-6,12-diol and chrysene-6,12-dione along angle β and the corresponding dihedral angle β' defined by carbon atoms 10, 10a, 10b and 11. These two compounds represent the electronic structure of the investigated systems lacking any strain. The results of these constrained optimisations are shown as contour plots in Figure 3.

The most notable observation is the large depth of the potential well of chrysene-6,12-diol. This corroborates the conclusion that the high energetic strain of the 6,12-dimethoxychrysene derivatives, as observed in Table 2, has its origin in the highly stable planar, aromatic chrysene core. The

Table 2. Strain energy of the 6,12-dimethoxychrysenes and chrysenes-6,12-dione derivatives calculated according to the homodesmotic reactions defined in Scheme 1. All energies are given in kJ mol^{-1} .

structure	BP86	B3LYP	BP86	B3LYP
reaction		(1)		(2)
2a	94.0	95.8	99.0	101.9
3a	95.2	101.0	110.9	115.2
4a	98.4	101.0	111.0	115.6
5a	92.6	93.4	111.3	114.0
reaction		(3)		(4)
7a	32.4	32.8	41.3	44.5
8a	37.6	38.7	45.8	48.9
9a	38.6	39.6	46.0	49.2
10a	56.6	62.7	66.6	74.9

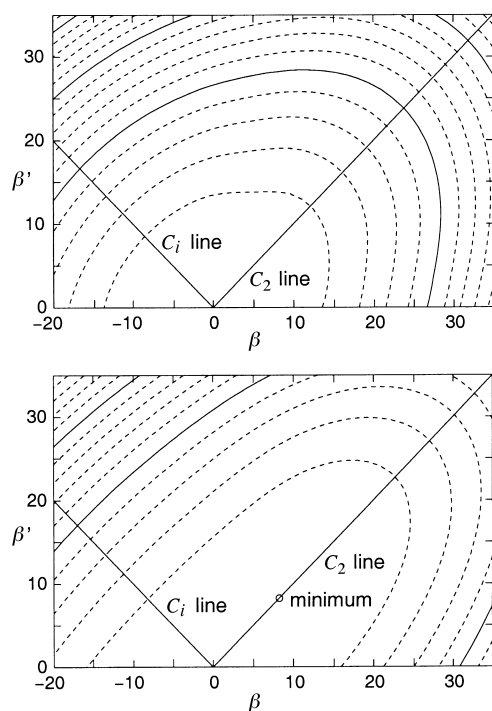


Figure 3. Two-dimensional cut along dihedral angles β and β' of the potential-energy surface of chrysenes-6,12-diol (top) and chrysenes-6,12-dione (bottom). Along the straight lines the indicated symmetry, C_2 or C_i , is preserved. The isoenergetic lines are separated by 2 kJ mol^{-1} . The lowest-energy structure for chrysenes-6,12-diol is at $\beta = \beta' = 0^\circ$.

second observation is that the distortion of the planar structures preserving C_2 symmetry follows a projected minimal gradient path for both compounds. This explains why the most stable structures of all investigated compounds exhibit C_2 rather than C_i symmetry. The comparatively flat potential curve of chrysenes-6,12-dione, which preserves C_2 symmetry, is the reason for the stronger twist of the chrysenes-6,12-dione derivatives relative to the 6,12-dimethoxychrysenes derivatives.

Conformational manifold: In the preceding section we noted that bending the substituents to the same or to opposite sides of the core can lead to minima with considerably different twisted cores for both of the two compound classes. It is clear that further conformational degrees of freedom are introduced by all substituents other than methyl. It is the subject of

this section to completely characterise the potential-energy surface, by also taking rotations around bonds of the substituents into account.

The carbon atoms of the alkyl substituent connected to atom C5 of the 6,12-dimethoxychrysenes or chrysenes-6,12-dione core are denoted by C_α , C_β , etc., and the ones of the alkyl substituent connected to atom C11 are denoted by $C_{\alpha'}$, $C_{\beta'}$, etc. We note that the alkyl groups can occupy only two principal conformations relative to the core with respect to a rotation around the C5– C_α or C11– $C_{\alpha'}$ bonds: axial and equatorial. Looking at the twisted structures along the line connecting atoms C5 and C11, the equatorial conformation is characterised by carbon atoms C_β and $C_{\beta'}$ pointing towards the concave side of the twisted core (cf. Figure 4). As a result

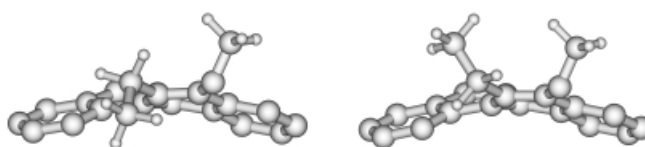


Figure 4. Minimum structures of **3** with the ethyl group in equatorial (left) and axial position (right). The hydrogen atoms of the chrysenes core as well as the substituent and the methoxy group on the back side have been omitted for clarity.

the C_α – C_β (or $C_{\alpha'}$ – $C_{\beta'}$) bond is close to coplanar with the plane defined by the core, hence the designation equatorial. As can be seen from Figure 1, this conformation is adopted by all lowest energy structures and thus seems to be favourable. The axial conformation, on the other hand, is characterised by carbon atoms C_β and $C_{\beta'}$ both pointing towards the convex side of the twisted core (cf. Figure 4). In this case the C_α – C_β and $C_{\alpha'}$ – $C_{\beta'}$ bond is nearly perpendicular to the plane defined by the core, hence it is denoted axial. In the case of the 6,12-dimethoxychrysenes derivatives we have to distinguish two close-lying axial conformations of the substituents in which the C_α – C_β bond exhibits different dihedral angles with the C5–C6 bond. Furthermore the two methoxy groups of the 6,12-dimethoxychrysenes derivatives can point not only to the same but also to opposite sides of the core, relative to the alkyl group attached to the neighbouring atom C5 or C11. Similar considerations hold both for the strongly twisted as well as the nearly planar conformers.

In the following a systematic approach is presented which allows the establishment of an exhaustive scan of the conformational manifold under consideration (cf. Table 3). Due to symmetry considerations it is sufficient, in the subsequent instructions, to take into account only the substituent and methoxy group of one of the inner rings and the corresponding phenanthrene substructure. We proceeded in our investigations taking the following steps:

- 1) Determination of the total number of conformational degrees of freedom (Table 3, column 2, designated as p). One degree of freedom is always given as the twisting motion of one of the phenanthrene substructures.
- 2) Estimation of the number of different minima each of the determined degrees of freedom can give rise to (column 3, designated as m_p). Test calculations can, of course, be necessary to confirm this estimate.

Table 3. Table for the determination of the maximal number of all theoretically conceivable conformers. p : total number of conformational degrees of freedom; m_p : number of different minima for each p ; tm : number of possible combinations of m_p ; tc : total number of conformers; nrc : number of nonredundant conformers.

structure	p	m_p	tm	tc	nrc
6,12-dimethoxychrysene derivatives					
2	2	2/2	4	16	6
3	3	2/2/3	12	144	42
4	4	2/2/3/3	36	1296	342
5	2	2/2	4	16	6
chrysene-6,12-dione derivatives					
7	1	2	2	4	2
8	2	2/2	4	16	6
9	3	2/2/3	12	144	42
10	1	2	2	4	2

3) Deduction of the number of possible combinations of the different individual conformations determined in step 2 (column 4, designated as tm). It is obtained as $tm = \prod_p m_p$. The total number of combinations in the molecule is obtained as the square of this number (column 5, designated as tc).

4) All possible conformers of the molecule can be described systematically by a square matrix, the row index of which represents all tm possible combinations deduced above and the column index of which represents the combinations of the substituent and methoxy group not considered in the steps above. In this representation all structures that exhibit C_2 symmetry are listed on the main diagonal, whereas all structures that exhibit C_i symmetry have entries on the diagonal from the lower left to the upper right corner of the matrix. All remaining elements represent structures with C_1 symmetry. The diagonal representing the structures with C_2 symmetry separates structures with symmetry-redundant conformations, whereas the diagonal representing the structures with C_i symmetry separates the enantiomers. Consequently only one of the four triangles defined by the diagonals of the matrix contains nonredundant conformers that have to be considered for electronic structure calculations. The maximal number of these conformers (column 6, designated as nrc) is given as $nrc = tm/2[(tm/2) + 1]$ for even tm values. Figure 5 gives the matrix of compound **2** as an example. It has the same form as the matrix for compounds **5** and **8**.

Table 3 contains the maximal number of conformers determined by this procedure for all compounds considered in this manuscript. It can, of course, turn out that some of these conformers do not exist in reality, simply because they exhibit a combination of conformations that is not stable. Test calculations are necessary to confirm or disprove the existence of each theoretically conceivable conformer.

As a result of the lack of the methoxy groups, all 5,11-disubstituted chrysene-6,12-dione derivatives have a significantly smaller amount of theoretically conceivable conformers. The carbonyl group is part of the core and does not have any influence on the conformational manifold. Apart from changing the electronic structure significantly it merely induces a small steric perturbation.

	aa'	ab'	ba'	bb'
aa	C_2	C_1	C_1	C_i
ab	C_1	C_2	C_i	C_1^*
ba	C_1	C_i	C_2^*	C_1^*
bb	C_i	C_1^*	C_1^*	C_2^*

Figure 5. Scheme for finding all theoretically conceivable conformers of compound **2**. The rows represent all possible combinations of conformations of the methyl substituent and methoxy group of one of the inner rings. The same information is given in the columns for the other methyl substituent and methoxy group. Labels a and b indicate that the methyl (or methoxy) group is located above or below the plane defined by the chrysene core. Changing the conformation of the methyl group from a to b is connected with a twisting motion of the corresponding phenanthrene substructure. The elements of the matrix denote the symmetry of the structure corresponding to the combination of conformations indicated by the row and column index. Enantiomers are labelled by asterisks, non-redundant conformers are highlighted by shaded matrix elements.

Racemisation pathways: Due to its large number of conformers we excluded 6,12-dimethoxy-5,11-dipropylchrysene (**4**) from further investigations. The excessive number of conformers originates from the possible combinations of rotations of the two propyl groups and is thus not of much interest. The only optimised propyl derivative is the most stable conformer **4a**, which was constructed in analogy to the most stable conformer of the ethyl derivative **3a**. Moreover, we did not investigate the transition state structures of 5,11-diethyl-6,12-dimethoxychrysene (**3**) and any structures, bar the most stable, of 5,11-dipropylchrysene-6,12-dione (**9**). It can be expected that these alkyl derivatives behave similarly to their smaller homologues. This is already indicated by the similarity of their equilibrium structures (cf. Figure 1 and Table 1).

6,12-Dimethoxy-5,11-dimethylchrysene: The topological map of the 6,12-dimethoxy-5,11-dimethylchrysene (**2**) conformational space is presented in Figure 6. Starting from **2a**, the

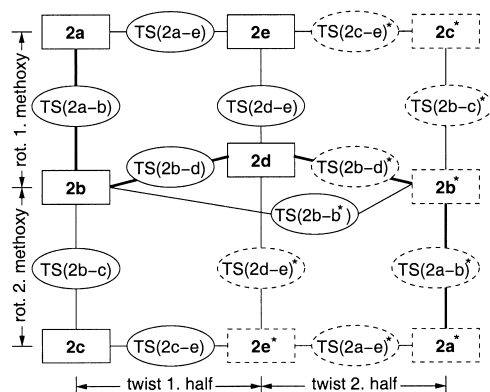


Figure 6. Topological map of the 6,12-dimethoxy-5,11-dimethylchrysene (**2**) conformational space. Dashed boxes indicate structures that have not been explicitly calculated; ellipses and the prefix TS indicate transition states; enantiomers are marked by asterisks. Structures contained in boxes and ellipses connected by vertical lines are converted into each other by rotations of a methoxy group, whereas those connected by horizontal lines are converted into each other via the more complex twisting motion of the chrysene core. The highlighted line from **2a** to **2a*** denotes the preferred racemisation pathway.

most stable conformer at the B3LYP level, both conformers resulting from the rotation of the methoxy groups (**2b** and **2c**) and the corresponding transition state structures (**TS(2a-b)** and **TS(2b-c)**) could be localised. It should be mentioned that the methoxy group is oriented towards the methyl substituent and not towards the outer benzene ring in these lower-lying transition states. Furthermore, two C_i -symmetrical conformers (**2e** and **2d**), resulting from a twisting motion of one of the phenanthrene substructures of the C_2 -symmetrical conformer **2a** and the C_1 -symmetrical conformer **2b**, respectively, turned out to be stable minimum structures. Due to the C_1 symmetry of conformer **2b**, it makes a difference which one of the two inequivalent phenanthrene substructures is involved in the twisting motion. As a consequence, another structure with C_i symmetry (**TS(2b-b*)**) is obtained by the corresponding twisting motion; this turned out to be a transition state. This way only five of the six theoretically conceivable conformers proved to be minima on the potential-energy surface.

The energetics of the structures are listed in Table 4. According to the density functional calculations, the preferred racemisation pathway between the most stable conformer **2a** and its enantiomer **2a*** involves the conformers **2b**, **2d** and **2b***. Thus the racemisation proceeds through a rotation of a methoxy group followed by a twisting motion of the phenanthrene substructure that has the rotated methoxy group attached. The rest of the racemisation pathway is enantiomeric to this first part. It turns out that the energy barrier of the twisting motion involved in the favoured racemisation pathway is only about one third of the energy barrier of the rotation of the methoxy group. The energy

diagram along the reaction path and corresponding structures is shown in Figure 7.

diagram along the reaction path and corresponding structures is shown in Figure 7.

To check for the reliability of the results obtained by the density functional calculations, we performed single-point MP2 calculations on the B3LYP structures involved in the most probable racemisation pathway. The results are listed in Table 4. Whereas the relative energies of the local minima are in nearly perfect agreement in all methods employed, the density functionals underestimate the energy barriers by an amount of about 5 kJ mol^{-1} , especially in the case of the twisting motion. This is in line with the well-known observation that B3LYP slightly underestimates barrier heights.^[25–27] Nevertheless, the relative height of the energy barrier of the rotation of the methoxy group and of the twisting motion is reproduced by the DFT calculations to a satisfactory extent. Thus we can conclude that density functional calculations are well suited to the estimation of the racemisation barriers of these compounds.

6,12-Dimethoxy-5,11-diphenylchrysene: The topological map of the 6,12-dimethoxy-5,11-diphenylchrysene (**5**) conformational space is presented in Figure 8. Starting from the most stable conformer **5a**, both conformers resulting from the

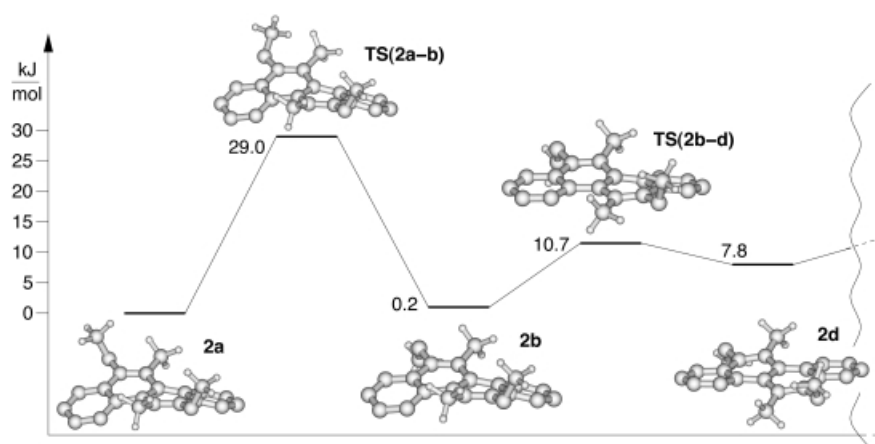


Figure 7. Energy diagram of the preferred racemisation pathway of 6,12-dimethoxy-5,11-dimethylchrysene (**2**) according to the B3LYP density functional results. Only the nonredundant part is shown. The hydrogen atoms of the chrysene core have been omitted for clarity. All energies are given in kJ mol^{-1} .

Table 4. Relative energies of all equilibrium and interconnecting transition state structures of 6,12-dimethoxy-5,11-dimethylchrysene (**2**). The total energy of **2a**, the most stable conformer at the B3LYP level, serves as reference. All energies are given in kJ mol^{-1} .

Structure	Symmetry	BP86	B3LYP	MP2
minima				
2a	C_2	0.0	0.0	0.0
2b	C_1	0.7	0.2	-0.7
2c	C_2	1.3	0.4	-1.6
2d	C_i	7.6	7.8	7.7
2e	C_1	12.9	13.9	16.9
transition states				
TS(2a-b)	C_1	25.4	29.0	34.4
TS(2b-c)	C_1	27.5	29.9	34.2
TS(2d-e)	C_1	36.8	40.2	44.1
TS(2b-d)	C_1	10.8	10.7	15.6
TS(2a-e)	C_1	13.3	14.1	15.7
TS(2c-e)	C_1	16.0	16.8	20.4
TS(2b-b*)	C_i	19.5	21.5	20.9

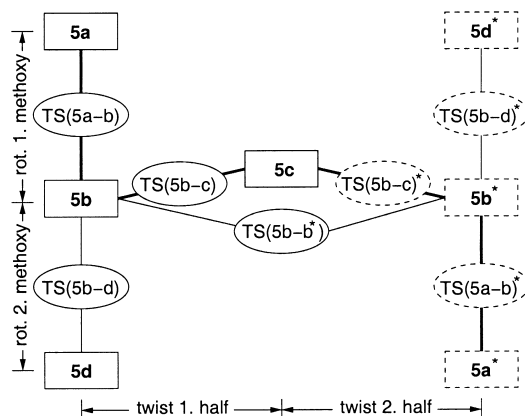


Figure 8. Topological map of the 6,12-dimethoxy-5,11-diphenylchrysene (**5**) conformational space. For an explanation see the caption of Figure 6.

rotation of the methoxy groups (**5b** and **5d**) and the corresponding transition state structures (**TS(5a-b)** and **TS(5b-d)**) could be localised, similar to the case of 6,12-dimethoxy-5,11-dimethylchrysene (**2**). Again, the methoxy group is oriented towards the substituent in these transition states, but only **5c** was found as a nearly planar semitwisted stable minimum structure resulting from a twisting motion of one of the phenanthrene substructures of **5b**. In conformer **5c** the neighbouring phenyl and methoxy groups are located on opposite sides of the plane defined by the chrysene core so that the strain energy is minimised. The C_i -symmetrical structure **TS(5b-b*)** resulting from the twisting motion of the other phenanthrene substructure of **5b** is a relatively high-lying transition state. It could only be obtained by symmetry-restricted optimisation. Thus only four of the six theoretically conceivable conformers turned out to be minima on the potential-energy surface.

The energetics of all structures are listed in Table 5. The most probable racemisation pathway shows similarities to that of 6,12-dimethoxy-5,11-dimethylchrysene (**2**). We find that the energy barrier of the twisting motion involved in the favoured racemisation pathway is only about half of the energy barrier of the rotation of the methoxy group.

Table 5. Relative energies of all equilibrium and interconnecting transition state structures of 6,12-dimethoxy-5,11-diphenylchrysene (**5**). The total energy of the most stable conformer **5a** serves as reference. All energies are given in kJ mol^{-1} .

Structure	Symmetry	BP86	B3LYP
minima			
5a	C_2	0.0	0.0
5b	C_1	13.0	13.5
5c	C_i	12.8	14.9
5d	C_2	25.4	26.3
transition states			
TS(5a-b)	C_1	22.5	26.7
TS(5b-d)	C_1	35.8	40.6
TS(5b-c)	C_1	16.2	17.6
TS(5b-b*)	C_i	27.4	29.3

5,11-Diethyl-6,12-dimethoxychrysene: Taking the two additional degrees of freedom resulting from rotations around the C5–Ca and C11–Ca' bonds into account, the manifold of conformers of this compound cannot be visualised in a simple two-dimensional scheme, as is the case for compounds **2** and **5**. We give, however, the energetics of the strongly twisted conformers in Table 6. The relative energies of these structures are in the range of 6–25 kJ mol^{-1} and, therefore, are comparable to the systems discussed before. It should be noted that no twisted conformer exists in which an ethyl substituent in an axial position is located close to a methoxy group that is pointing to the same side of the plane defined by the chrysene core. It was possible to put the conformers into correspondence with those conformers of **2**, which, without taking the additional rotational degrees of freedom of **3** into account, have identical conformations. Further investigation of the flat semitwisted structures was not carried out, since it seems evident that the results would agree with those obtained for **2**. It is very likely that the preferred racemisation

Table 6. Relative energies of all twisted conformers of 6,12-dimethoxy-5,11-diethylchrysene (**3**) and their correspondence with the equilibrium structures of 6,12-dimethoxy-5,11-dimethylchrysene (**2**). The total energy of the most stable conformer **3a** serves as reference. All energies are given in kJ mol^{-1} .

Structure	Symmetry	2 ^[a]	BP86	B3LYP
3a	C_2	2a	0.0	0.0
3b	C_1	2a	6.5	6.4
3c	C_1	2b	7.3	7.3
3d	C_1	2b	8.0	8.0
3e	C_1	2b	12.2	12.2
3f	C_2	2a	12.4	12.3
3g	C_1	2b	13.5	13.5
3h	C_1	2c	19.3	19.3
3i	C_1	2c	15.7	15.6
3j	C_2	2c	15.7	15.6
3k	C_1	2b	20.8	20.8
3l	C_2	2c	16.7	16.6
3m	C_1	2c	20.9	20.9
3n	C_2	2c	24.7	24.7

[a] Corresponding derivatives of **2**.

pathway of **3** will involve a rotation of the methoxy and neighbouring ethyl group followed by a twisting motion of the phenanthrene substructure that has those groups on an outer ring, leading to a semitwisted C_i -symmetrical structure, as is the case for **2**.

5,11-Dimethylchrysene-6,12-dione: The topological map of the 5,11-dimethylchrysene-6,12-dione (**7**) conformational space is shown in Figure 9, with the energetics of all structures

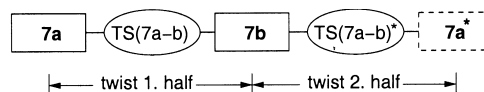


Figure 9. Topological map of the 5,11-dimethylchrysene-6,12-dione (**7**) conformational space. For an explanation see the caption of Figure 6.

listed in Table 7. Both of the two theoretically conceivable conformers could be found. One is the twisted equilibrium structure **7a** with C_2 symmetry. The other one (**7b**), being C_i -symmetrical, has a nearly planar chrysene core, with the methyl groups pointing to opposite sides of the plane defined by the core. Both the structure and the energy of the transition state **TS(7a-b)** are very similar to conformer **7b**. This means that the molecule will flip very rapidly between the enantiomers **7a** and **7a***.

Table 7. Relative energies of all equilibrium and interconnecting transition state structures of 5,11-dimethylchrysene-6,12-dione (**7**). The total energy of the most stable conformer **7a** serves as reference. All energies are given in kJ mol^{-1} .

Structure	Symmetry	BP86	B3LYP
minima			
7a	C_2	0.0	0.0
7b	C_i	24.2	27.8
transition state			
TS(7a-b)	C_1	24.5	28.1

5,11-Diphenylchrysene-6,12-dione: The topological map of the 5,11-diphenylchrysene-6,12-dione (**10**) conformational space is shown in Figure 10, along with the energetics of all structures in Table 8. Similarly to compound **7**, two conformers exist. Of course, the symmetries of these conformers coincide with those of **7** as well. As in the case of compound **7**, the energy of the transition state **TS(10a-b)** is very similar to the energy of conformer **10b**.

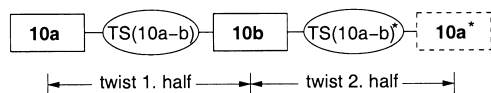


Figure 10. Topological map of the 5,11-diphenylchrysene-6,12-dione (**10**) conformational space. For an explanation see the caption of Figure 6.

Table 8. Relative energies of all equilibrium and interconnecting transition state structures of 5,11-diphenylchrysene-6,12-dione (**10**). The total energy of the most stable conformer **10a** serves as reference. All energies are given in kJ mol^{-1} .

Structure	Symmetry	BP86	B3LYP
minima			
10a	C_2	0.0	0.0
10b	C_i	15.7	21.7
transition state			
TS(10a-b)	C_1	17.7	21.9

The rotational degree of freedom around the C5–Ca or C11–Ca' bond is strongly coupled to the twisting motion of the scaffold. The position of the phenyl group is determined by the twist of the chrysene core. Another point of view would be that a rotation of the phenyl group around the C5–Ca or C11–Ca' bond induces a twisting motion of the associated phenanthrene substructure of the chrysene core.

5,11-Diethylchrysene-6,12-dione: The topological map of the 5,11-diethylchrysene-6,12-dione (**8**) conformational space is shown in Figure 11. This compound has the same pattern of conformational degrees of freedom as 6,12-dimethoxy-5,11-diphenylchrysene (**5**), so for both sides of the chrysene core there are two degrees of freedom, each allowing two possible positions, and a similar topology occurs. Starting from the

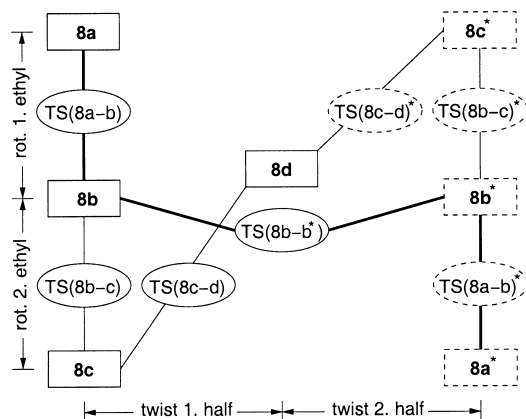


Figure 11. Topological map of the 5,11-diethylchrysene-6,12-dione (**8**) conformational space. For an explanation see the caption of Figure 6.

most stable conformer **8a**, both conformers resulting from the rotation of the ethyl groups (**8b** and **8c**) and the corresponding transition state structures (**TS(8a-b)** and **TS(8b-c)**) could be localised. It should be mentioned that the ethyl substituent is oriented towards the oxo group and not towards the outer benzene ring in these lower-lying transition states. Two C_i -symmetrical structures are also obtained. While **8d** turned out to be a stable conformer, **TS(8b-b*)** is a transition state.

The energetics of all conformers are listed in Table 9. According to Table 9, the preferred racemisation pathway between the most stable conformer **8a** and its enantiomer **8a*** involves only the conformer **8b**. We could not localise any

Table 9. Relative energies of all equilibrium and interconnecting transition state structures of 5,11-diethyl-6,12-dimethoxychrysene (**8**). The total energy of the most stable conformer **8a** serves as reference. All energies are given in kJ mol^{-1} .

Structure	Symmetry	BP86	B3LYP
minima			
8a	C_2	0.0	0.0
8b	C_1	5.9	6.1
8c	C_2	12.1	12.6
8d	C_i	35.8	40.6
transition states			
TS(8a-b)	C_1	35.1	35.1
TS(8b-c)	C_1	40.9	40.9
TS(8b-b*)	C_i	34.5	40.2
TS(8c-d)	C_1	46.2	49.4

transition state of a twisting motion that converts **8b** into **8d**. Rotation of the second ethyl group leading to **8c**, followed by a twisting motion that is coupled to a rotation of the ethyl group connected to the outer benzene ring of the associated phenanthrene substructure, seems to be the only way which leads to **8d**. In any case it is more favourable to involve both phenanthrene substructures in the twisting motion and thus directly arrive at conformer **8b*** by passing the transition state **TS(8b-b*)**. The energy barrier of the twisting motion involved in the favoured racemisation pathway is as big as the energy barrier of the rotation of the ethyl substituent.

Conclusion

Our calculations show that the strain energy and the energy barriers of the rotations and the twisting motion are of the same order of magnitude. Thus, rotation of substituents and the twisting motion of the chrysene scaffold are equally important in the racemisation process. Due to the aromaticity of the core of the 6,12-dimethoxychrysene derivatives, their most stable equilibrium structures are distorted to a lesser degree than those of the corresponding chrysene-6,12-dione derivatives. From another point of view, the sterically demanding substituents of the chrysene-6,12-dione derivatives can avoid repulsive interaction by twisting the core more easily. Consequently, the strain energy of the 6,12-dimethoxychrysene derivatives is at least a factor of two larger, with the aromaticity being responsible again. The different electronic structures of the two investigated compound classes do not

have a major influence on the racemisation barriers. For each compound we could localise at least one of the nearly planar semitwisted conformers, and the favoured racemisation pathway involves one of these structures in all cases except for 5,11-diethylchrysene-6,12-dione (**8**). Thus, the twisting motion takes place in two steps in all but one of the investigated cases. However, it must be taken into account that, particularly in the case of the chrysene-6,12-dione derivatives, the potential-energy surface in the region of these semitwisted structures proved very flat. Thus any possibility of finding a way to isolate or intercept the semitwisted structures seems unlikely. It is clear that compounds with larger alkyl substituents require further rotations to reach their corresponding enantiomer. The activation barriers of these rotations are of the magnitude of the rotation barriers in alkanes and therefore are not expected to be of importance.

Acknowledgement

We gratefully acknowledge support by the Deutsche Forschungsgemeinschaft in the framework of SFB334, and in part by the Fonds der Chemischen Industrie.

- [1] K. H. Dötz, Th. Schäfer, F. Kroll, K. Harms, *Angew. Chem.* **1992**, *104*, 1257–1259; *Angew. Chem. Int. Ed. Engl.* **1992**, *31*, 1236–1238.
- [2] F. Hohmann, S. Siemoneit, M. Nieger, S. Kotila, K. H. Dötz, *Chem. Eur. J.* **1997**, *3*, 853–859.
- [3] S. Grimme, S. D. Peyerimhoff, *Chem. Phys.* **1996**, *204*, 411–417.
- [4] S. Grimme, H. G. Löhmannsröben, *J. Phys. Chem.* **1992**, *96*, 7005–7009.
- [5] R. N. Armstrong, D. A. Lewis, *J. Org. Chem.* **1985**, *50*, 907–908.
- [6] R. N. Armstrong, H. L. Ammon, J. N. Dranow, *J. Am. Chem. Soc.* **1987**, *109*, 2077–2082.
- [7] A. I. Kitaigorodskii, V. G. Dashevskii, *Tetrahedron* **1968**, *24*, 5917–5928.
- [8] J. Kao, N. L. Allinger, *J. Am. Chem. Soc.* **1977**, *99*, 975–986.
- [9] R. Fritsch, E. Hartmann, D. Andert, A. Mannschreck, *Chem. Ber.* **1992**, *125*, 849–855.
- [10] R. Ahlrichs, M. Bär, M. Häser, H. Horn, C. Kölmel, *Chem. Phys. Lett.* **1989**, *162*, 165–169.
- [11] A. D. Becke, *Phys. Rev. A* **1988**, *38*, 3098–3100.
- [12] J. P. Perdew, *Phys. Rev. B* **1986**, *33*, 8822–8824.
- [13] A. D. Becke, *J. Chem. Phys.* **1993**, *98*, 5648–5652.
- [14] K. Eichkorn, O. Treutler, H. Öhm, M. Häser, R. Ahlrichs, *Chem. Phys. Lett.* **1995**, *242*, 652–660.
- [15] K. Eichkorn, F. Weigend, O. Treutler, R. Ahlrichs, *Theor. Chem. Acc.* **1997**, *97*, 119–124.
- [16] F. Weigend, M. Häser, *Theor. Chem. Acc.* **1997**, *97*, 331–340.
- [17] F. Weigend, M. Häser, H. Patzelt, R. Ahlrichs, *Chem. Phys. Lett.* **1998**, *294*, 143–152.
- [18] A. Schäfer, C. Huber, R. Ahlrichs, *J. Chem. Phys.* **1994**, *100*, 5829–5835.
- [19] C. Kind, M. Reiher, J. Röder, B. A. Hess, *Phys. Chem. Chem. Phys.* **2000**, *2*, 2205–2210.
- [20] S. Grimme, M. Gastreich, NUMFREQ, Parallel implementation of frequency analysis based on numerical derivatives of analytical gradients, University of Bonn, Bonn (Germany), **1998**.
- [21] J. Neugebauer, M. Reiher, C. Kind, B. A. Hess, *J. Comp. Chem.* **2002**, *23*, 895–910.
- [22] C. Kind, ROTCURVE, Program for the computation of reaction coordinates using TURBOMOLE, University of Erlangen-Nürnberg, Erlangen (Germany), **2000**.
- [23] G. Schaftenaar, MOLDEN, CAOS/CAMM Center Nijmegen, Toernooiveld, Nijmegen (The Netherlands), **1991**.
- [24] P. George, M. Trachtman, C. W. Bock, A. M. Brett, *Theoret. Chim. Acta* **1975**, *38*, 121–129.
- [25] B. S. Jursic, *Chem. Phys. Lett.* **1996**, *256*, 603–608.
- [26] B. J. Lynch, D. G. Truhlar, *J. Phys. Chem. A* **2001**, *105*, 2936–2941.
- [27] J. K. Kang, C. B. Musgrave, *J. Chem. Phys.* **2001**, *115*, 11040–11051.

Received: September 2, 2002 [F4383]